

# 3D Software Synthesis Guided by Constraint-Expressive Intermediate Representation

Shuqing Li

The Chinese University of Hong Kong  
Hong Kong, China  
sqli21@cse.cuhk.edu.hk

Anson Y. Lam

The Chinese University of Hong Kong  
Hong Kong, China  
yflam@link.cuhk.edu.hk

Yun Peng

The Chinese University of Hong Kong  
Hong Kong, China  
ypeng@cse.cuhk.edu.hk

Wenxuan Wang

Renmin University of China  
Beijing, China  
wangwenxuan@ruc.edu.cn

Michael R. Lyu

The Chinese University of Hong Kong  
Hong Kong, China  
lyu@cse.cuhk.edu.hk

## Abstract

Graphical user interface (UI) software has undergone a fundamental transformation from traditional two-dimensional (2D) desktop/web/mobile interfaces to spatial three-dimensional (3D) environments. While existing work has made remarkable success in automated 2D software generation, such as HTML/CSS and mobile app interface code synthesis, the generation of 3D software still remains under-explored. Current methods for 3D software generation usually generate the 3D environments as a whole and cannot modify or control specific elements in the software. Furthermore, these methods struggle to handle the complex spatial and semantic constraints inherent in the real world.

To address the challenges, we present SCENETHESIS, a novel requirement-sensitive 3D software synthesis approach that maintains formal traceability between user specifications and generated 3D software. SCENETHESIS is built upon SCENETHESISLANG, a domain-specific language that serves as a granular constraint-aware intermediate representation (IR) to bridge natural language requirements and executable 3D software. It serves both as a comprehensive scene description language enabling fine-grained modification of 3D software elements and as a formal constraint-expressive specification language capable of expressing complex spatial constraints. By decomposing 3D software synthesis into stages operating on SCENETHESISLANG, SCENETHESIS enables independent verification, targeted modification, and systematic constraint satisfaction. Our evaluation demonstrates that SCENETHESIS accurately captures over 80% of user requirements and satisfies more than 90% of hard constraints while handling over 100 constraints simultaneously. Furthermore, SCENETHESIS achieves a 42.8% improvement in BLIP-2 visual evaluation scores compared to the state-of-the-art method, establishing its effectiveness in generating high-quality 3D software that faithfully adheres to complex user requirements.

## ACM Reference Format:

Shuqing Li, Anson Y. Lam, Yun Peng, Wenxuan Wang, and Michael R. Lyu. 2018. 3D Software Synthesis Guided by Constraint-Expressive Intermediate Representation. In *Proceedings of Make sure to enter the correct conference title from your rights confirmation email (Conference acronym 'XX)*. ACM, New York, NY, USA, 13 pages. <https://doi.org/XXXXXXXX.XXXXXXX>

## 1 Introduction

Graphical user interface (UI) software has been a cornerstone of computing since the introduction of the Xerox Alto in 1973 [57], initially manifesting as two-dimensional (2D) interfaces that revolutionized human-computer interaction. The software engineering (SE) community has developed mature ecosystems and techniques for automated 2D UI generation [22, 23, 54, 58, 65, 80], including model-based approaches, template-driven synthesis, and constraint-based layout algorithms. Driven by advances in graphics hardware and the emergence of 3D engines, such as Unity, since the early 2000s, three-dimensional (3D) software has experienced explosive growth. The global 3D software market reached more than 32 billion in 2024 [1], spanning many domains such as robotics simulators, training platforms for autonomous (aerial) vehicles, 3D games, virtual production systems, modeling and design applications, digital twin platforms, and extended reality (VR/AR) applications. Despite the rapid growth of 3D software, the automated synthesis of 3D software still remains underexplored.

The established methods for 2D UI generation cannot be directly applied to 3D software synthesis due to fundamental differences in spatial complexity, physical constraints, and interaction paradigms. Recent end-to-end text-to-3D generation approaches propose directly generating complete 3D software from natural language (NL) based on neural synthesis [26, 31], procedural modeling [13], or constraint-based methods [73]. They typically regard 3D software generation as a monolithic vision problem rather than a structured software synthesis task. However, high-quality 3D software should not only be visually compelling but also functionally correct, physically plausible, and programmatically testable. These approaches lack fine-grained intermediate representations (IRs) that bridge the semantic gap between high-level requirements and low-level 3D software implementations. Without such IRs, these approaches operate as black boxes that directly map NL to 3D outputs, making it impossible to inspect, verify, or modify the generation process.

Permission to make digital or hard copies of all or part of this work for personal or classroom use is granted without fee provided that copies are not made or distributed for profit or commercial advantage and that copies bear this notice and the full citation on the first page. Copyrights for components of this work owned by others than the author(s) must be honored. Abstracting with credit is permitted. To copy otherwise, or republish, to post on servers or to redistribute to lists, requires prior specific permission and/or a fee. Request permissions from [permissions@acm.org](mailto:permissions@acm.org).  
*Conference acronym 'XX, June 03–05, 2018, Woodstock, NY*

© 2018 Copyright held by the owner/author(s). Publication rights licensed to ACM.  
ACM ISBN 978-1-4503-XXXX-X/18/06  
<https://doi.org/XXXXXXXX.XXXXXXX>

Some recent work [73] pioneered the use of intuitive IR, such as scene graphs, to capture users' requirements. While intuitive, scene graphs restrict object classes to predefined categories and relationships to a few discrete types (typically only *left/right/top/down*), which fundamentally limits their expressiveness. Moreover, the assumption of at most one relation between two objects makes it impossible to express complex spatial constraints for real-world applications. In summary, it lacks a systematic approach with typical SE principles to generate controllable, verifiable, and maintainable 3D software.

Specifically, current approaches to 3D software synthesis face the following challenges:

**Challenge 1 (C1): Lack of Compositional Control and Post-Generation Maintainability.** Current methods generate 3D software as a whole and do not support modification of specific elements in 3D scenes. The lack of controllability over specific elements makes it quite challenging to meet precise specifications, as current methods have to regenerate the entire software in each iteration to fix even minor errors. For example, a single misplaced object or violated constraint requires regenerating the entire software from scratch. This is a fundamental violation of SE principles of predictability and control. Furthermore, when specifications evolve or bugs are discovered in deployed 3D software, developers cannot perform targeted fixes or incremental updates. The absence of expressive IRs between requirements and final 3D software fundamentally prevents developers from tracing the rationale behind specific design decisions and maintaining version control at the component level.

**Challenge 2 (C2): Inability to Handle Complex Constraints.** Real-world 3D software systems require satisfying diverse spatial, semantic, and physical constraints. For instance, a robot testing environment might require “*all emergency equipment must be accessible within 2 meters of any workstation while maintaining clear 1.5-meter evacuation paths.*” Current methods cannot reliably encode or verify such domain-specific requirements. Structure-based approaches like InstructScene [41] employ “scene graphs” to illustrate the complex constraints, but they suffer from severe expressiveness limitations. Scene graphs incorporate only simple and fixed spatial relationship categories, such as “left” and “above”, to describe the constraints between objects, so they can hardly capture the complicated continuous spatial relationships required by the constraints in the specifications.

To address these challenges, we present SCENETHESIS, a novel UI code synthesis system for 3D software environments. It is built upon SCENETHESISLANG, a domain-specific language (DSL) that serves as both a comprehensive 3D software scene description language to enable the modification of specific elements in software (C1), and a spatial constraint specification language to handle complex constraints in requirements (C2). SCENETHESISLANG acts as a more expressive IR that maintains interpretability while supporting continuous values and simultaneous relationships. Our approach fundamentally reimagines 3D software synthesis through an SE lens, decomposing the complex problem into four distinct, verifiable stages that collectively ensure both correctness and tractability:

**Requirement Formalization:** SCENETHESIS translates NL requirements into formal SCENETHESISLANG specifications, establishing unambiguous semantics for all software assets (i.e., objects in

3D environments) and spatial relationships. SCENETHESISLANG also encodes implicit physical laws that are often overlooked by users in the requirements but must be followed to make the generated software scenes both physically plausible and functionally correct.

**Asset Synthesis:** SCENETHESIS transforms object declarations from SCENETHESISLANG specifications into concrete 3D models through a hybrid strategy, which balances the retrieval of existing models from curated databases and the text-to-3D generation of new models. This strategy ensures both quality and coverage.

**Spatial Constraint Solving:** By formulating object placement as a constraint satisfaction problem over continuous 3D space, we design a novel Rubik Spatial Constraint Solver that employs an iterative refinement approach inspired by Rubik's cube solving, where local adjustments propagate to achieve global constraint satisfaction. This method provides strong guarantees about constraint satisfaction and remains computationally tractable even for complex scenarios.

**Software Synthesis:** The final stage combines solved object layouts with acquired 3D models to produce executable Unity-compatible software artifacts. They provide clear APIs for programmatic manipulation, embedded metadata for traceability, and support for round-trip engineering.

This modular, inspectable generation pipeline provides transparency and control at each step, allowing developers to inspect intermediate representations and modify specific components without full regeneration. SCENETHESISLANG enables developers to express arbitrary spatial, physical, and semantic constraints using a rich algebra of operations and predicates. It also moves beyond the categorical limitations of scene graphs (the intuitive IR used by existing work) to support continuous values, multiple simultaneous relationships, and complex logical compositions.

To evaluate SCENETHESIS, we construct a dataset consisting of 50 highly comprehensive user queries, with an average length of 508.4 words per query, which is approximately the number of words that fit on an A4 page with default formatting, spanning a diverse spectrum of room types. Evaluation results show that SCENETHESIS can accurately capture more than 80% of user requirements even when the threshold is relatively high, and that it can satisfy over 90% of hard constraints while handling more than 100 constraints. In terms of visual scores, SCENETHESIS outperforms all baselines (end-to-end LLM and Holodeck [73]) across all metrics under different LLM backbones, and even achieves a BLIP-2 [32] evaluation score that is 42.8% higher than current state-of-the-art, Holodeck [73].

The primary contributions of this work are:

- A formal DSL for 3D scenes that unifies spatial constraint specification with scene description, providing both expressiveness and verifiability for 3D software generation.
- A principled four-stage synthesis pipeline that decomposes 3D scene generation into requirement formalization, asset synthesis, spatial constraint solving, and software synthesis, with each stage independently verifiable and modular.
- A novel iterative constraint-solving algorithm that avoids the exponential complexity of traditional approaches through local-to-global refinement, achieving practical scalability for complex 3D software.

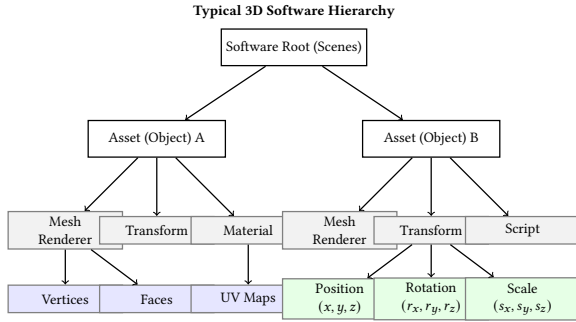


**Figure 1: Typical hierarchical structure of 3D software.** Each asset (object) serves as a container for components that define behavior and appearance. Mesh renderers contain the geometric data (vertices, faces), while transforms specify spatial properties in 3D space.

- Comprehensive evaluation demonstrating the superior effectiveness of SCENETHESIS compared with existing baselines.

## 2 Preliminaries

**3D Software.** As shown in Figure 1, 3D software systems represent virtual environments through a hierarchical structure [16]. A 3D model consists of three components: (1) *Geometry*: meshes comprising vertices, edges, and faces that define surface structure; (2) *Appearance*: materials specifying textures, colors, and shaders for visual rendering; (3) *Spatial Properties*: transforms encoding position  $(x, y, z)$ , rotation  $(r_x, r_y, r_z)$ , and scale  $(s_x, s_y, s_z)$  in 3D space. A scene comprises multiple models in a shared coordinate system. We adopt a left-handed system where (1)  $x$ ,  $y$ , and  $z$  axes represent width, height, and depth respectively, (2) the front of an unrotated object should be facing the positive  $z$ -axis, and (3) the order of rotation is  $x \rightarrow z \rightarrow y$ . Unity [56], our target platform, organizes content through GameObjects containing components (mesh renderers, colliders, scripts) that define 3D software entities.

**Spatial Constraints.** Professional 3D software must satisfy three constraint categories: *Geometric constraints* specify spatial relationships (e.g., "A is 2m from B":  $\|pos_A - pos_B\|_2 = 2.0$ ). *Physical constraints* ensure plausibility through collision avoidance and gravity support. *Semantic constraints* encode domain rules (e.g., "emergency exits must be accessible").

## 3 Approach: SCENETHESIS

This section presents the technical details of SCENETHESIS, a constraint-driven synthesis framework that transforms NL requirements into executable 3D software. Figure 2 shows the overview of SCENETHESIS. Our approach fundamentally differs from existing end-to-end generation methods by introducing SCENETHESISLANG as a formal intermediate representation that bridges the semantic gap between user intentions and implementable 3D scenes.

### 3.1 Overview and Design Principles

The core architectural principle of SCENETHESIS is to decompose the complex problem of 3D scene synthesis into four distinct, verifiable stages that collectively ensure both correctness and tractability.

This decomposition follows several typical software engineering principles: (1) **Modularity**: each stage can be developed, tested, and improved independently; (2) **Inspectability**: intermediate representations are human-readable and machine-verifiable; (3) **Correctness**: formal specifications enable systematic verification of generated scenes; and (4) **Controllability**: developers can intervene at any stage to refine or redirect the synthesis process.

Our four-stage pipeline operates as follows: Given an NL query  $Q$  describing the desired 3D environment, SCENETHESIS first performs **Requirement Formalization** (Stage I) to translate  $Q$  into a precise SCENETHESISLANG specification  $S$ . Next, **Asset Synthesis** (Stage II) processes the asset (3D object) declarations in  $S$  to obtain concrete 3D models  $M = \{m_1, m_2, \dots, m_n\}$ . Then comes **Spatial Constraint Solving** (Stage III), which formulates the placement of objects as a constraint satisfaction problem (CSP) over continuous 3D space and employs a novel Rubik Spatial Constraint Solver to perform iterative twist-and-fix and find the valid object transforms  $T = \{t_1, t_2, \dots, t_n\}$ . Finally, **Software Synthesis** (Stage IV) combines  $M$  and  $T$  to generate executable 3D software.

Throughout this framework, SCENETHESISLANG serves as both constraint language and 3D software description language. SCENETHESISLANG serves as the single source of truth, providing formal semantics for all spatial relationships and enabling systematic verification of constraint satisfaction. The formalization process makes implicit physical laws explicit (e.g., gravity, collision avoidance) while preserving user-specified requirements, ensuring that generated scenes are both physically plausible and functionally correct.

### 3.2 Stage I: Requirement Formalization

The first stage transforms ambiguous NL input into a precise, verifiable specification in SCENETHESISLANG. This formalization process serves two critical goals: establishing unambiguous semantics for all requirements and inferring hidden physical constraints.

**3.2.1 Natural Language Analysis and Contextualization.** Given a user query  $Q$ , we first perform semantic analysis to determine the scene context and extract structured information. We employ a large language model (LLM) with few-shot prompting to classify the scene type (indoor vs. outdoor), which determines the applicable constraint templates and default assumptions. For instance, indoor scenes automatically inherit boundary constraints (objects must remain within walls) and require ceiling/floor specifications, while outdoor scenes assume unbounded horizontal space.

SCENETHESIS then performs **controlled prompt expansion** based on LLMs to enrich the description with contextual details, since user requirements usually contain hidden constraints. For example, the user requirement "a modern conference room" contains hidden requirements for the furniture arrangements, lighting conditions, and accessibility. The expansion is strictly constrained to preserve all explicit user requirements while adding plausible hidden constraints inferred from the user requirements. Formally, let  $Q'$  denote the expanded prompt where  $Q' = Q \cup \{c_1, c_2, \dots, c_k\}$  such that each  $c_i$  represents an inferred contextual constraint from  $Q$ . Next, sub-prompt  $Q'_i$  ( $i \in \{1, \dots, r\}$  where  $r$  is the number of regions) for region  $i$  is generated via another LLM call by extracting sentences in  $Q'$  that are relevant via region  $i$ . In the following stages,

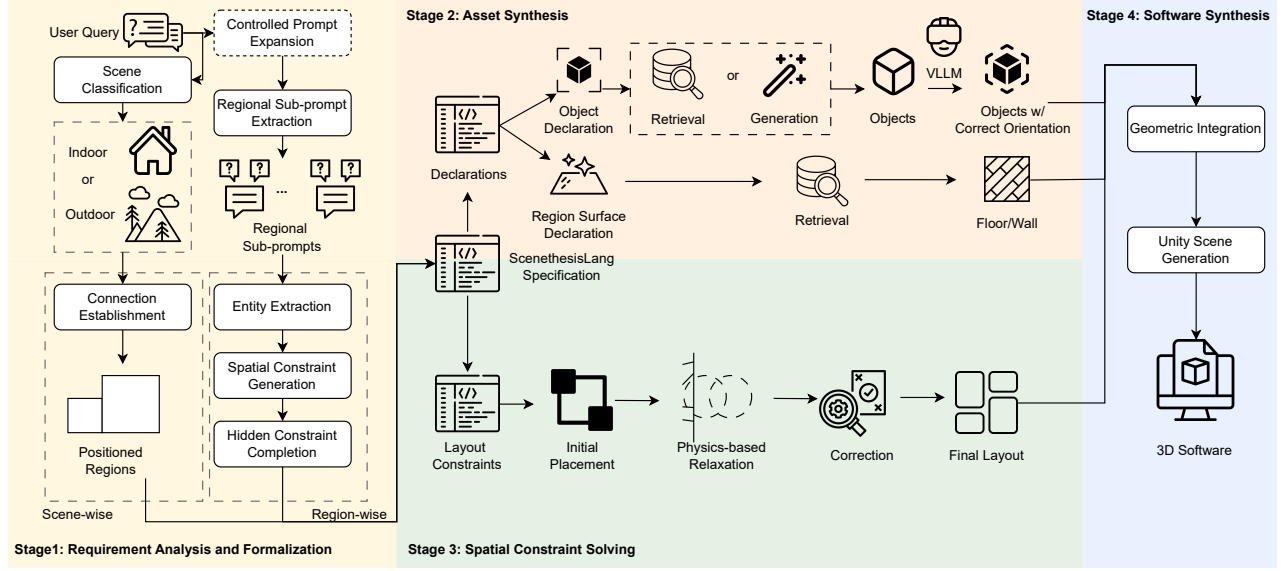


Figure 2: Overview of SCENETHESIS

$program \in Programs ::= stmt;   stmt; program$	(1)
$stmt \in Statements ::= decl   const   assign$	(2)
$decl \in Declarations ::= object\ id   region\ id   \tau\ id$	(3)
$const \in Constraints ::= assert\ \phi   allowCollide(id, id)   allowOutside(id)$	(4)
$assign \in Assignments ::= id.\alpha \leftarrow e   id.\beta \leftarrow e   id \leftarrow e$	(5)
$\alpha \in Object\ Properties ::= color   material   features$	(6)
$\beta \in Region\ Properties ::= pos   rot   scale  $	(7)
$\phi \in Assertions ::= e \triangleright e   inside(id, id)   \phi \wedge \phi   \phi \vee \phi   \neg\phi$	(8)
$\tau \in Types ::= Number   Degree   Bool   Vector3$	(9)
$  Rotation   Color   Material$	(10)
$e \in Expressions ::= n   id   s   e \odot e$	(11)
$  rand(e, e)   vec3(e, e, e)   rot(e, e, e)$	(12)
$  dot(e, e)   id.p$	(13)
$\triangleright \in Compare\ Operators ::= =   \neq   <   \leq   >   \geq$	(14)
$\odot \in Arithmetic\ Operators ::= +   -   *   /$	(15)
$n \in Numbers ::= any\ number$	(16)
$s \in Strings ::= any\ string$	(17)
$id \in Identifiers ::= names\ of\ the\ objects,\ regions\ and\ variables$	(18)

Figure 3: Domain-specific language: SCENETHESISLANG

scene-wise processing and generation use  $Q'$  while region-wise processing and generation use  $Q'_i$ .

**3.2.2 DSL Specification Generation.**  $Q'$  and  $Q'_i$  are then translated into a formal SCENETHESISLANG program consisting of declarations, constraints and assignments. Figure 3 presents the specification for SCENETHESISLANG. With object declaration statements, SCENETHESISLANG is able to describe each object in the scenes separately for stronger controllability. With constraint statements, SCENETHESISLANG could describe the arbitrary spatial relationships between objects to facilitate complex constraint solving.

Scene-wise, SCENETHESIS first establishes connections between regions based on semantic information stored in  $Q'$ . If the scene is indoor, the category (type of door or window), description, and

dimensions of each connection object are also generated. SCENETHESIS then proceeds to region positioning in which an LLM is asked to generate the vertices of each region conditioned on the previously established pairs of connections. To further improve realism, unlike previous work [73], we want walls in indoor scenes to have some thickness  $\eta$  instead of being just a piece of paper. To this end, we begin by shifting the vertices of each region horizontally (the direction and amount to shift is outputted by an LLM) so that the distance between every neighboring pair is exactly  $2\eta$  units. Then, when we are creating a mesh for each region in a later stage, we use Blender to extend the walls outward by  $\eta$  units.

Region-wise, given  $Q'_i$ , SCENETHESIS conducts three steps to build the SCENETHESISLANG program:

**Step 1: Entity Extraction.** SCENETHESIS first extracts all entities mentioned in  $Q'_i$  and creates an object declaration statement for each entity, i.e., **entity**  $id$ . Each entity in SCENETHESISLANG has three properties, *color*, *material* and *features*, to describe the details of the entity. These entities can be divided into two types: region surface textures (floor and walls) and objects. Each object has two additional properties, namely, category and dimensions.

**Step 2: Spatial Constraint Generation.** Given the extracted objects, SCENETHESIS then captures the NL descriptions about the spatial relationships among the objects. For each captured spatial relationship, SCENETHESIS creates a constraint statement in SCENETHESISLANG with the help of LLM to describe it. For instance, “the lamp hangs above the table” becomes a constraint statement:

$$assert\ lamp.pos.y > table.pos.y + table.scale.y$$

To reduce the chance of having redundant or contradictory subsets in the generated set of constraint statements (a set of constraints is redundant if keeping only one constraint in this set will not change the overall physical meaning of the scene, while a set of constraints is contradictory if satisfying one constraint in this set implies that other constraints in the same set can never be satisfied), we first pass the set to an LLM at most  $v_r$  times to identify and

remove redundant subsets, and then pass the resulting set to an LLM at most  $v_c$  times to identify and remove contradictory subsets.

**Step 3: Hidden Constraint Completion.** SCENETHESIS lastly adds physical realism constraints to make sure that the generated scene follows the sense of the physical world. For example, we add a constraint for all objects to ensure that they do not collide with each other unless allowed:

$$\forall o_i, o_j \in \mathcal{O}, i \neq j \Rightarrow \neg \text{collides}(o_i, o_j) \vee \text{allowCollide}(o_i, o_j)$$

Similarly, we also add gravity constraints to ensure proper support relationships, and boundary constraints to keep objects within designated regions unless explicitly overridden.

### 3.3 Stage II: Asset Synthesis

Instead of generating the entire scene, SCENETHESIS generates each object independently to ensure high controllability and facilitate easier fixes for small errors. The second stage processes object declarations from the SCENETHESISLANG specification to obtain concrete 3D models. This stage operates independently on each object, enabling parallel processing and modular replacement of acquisition strategies.

**3.3.1 Query Formulation.** For an object, the query is formulated as “a 3D model of a <color> <category> made with <material> that is <features>”. For a region surface texture, the query is formulated as “a <color> floor/wall made of <material> that is <features>”. Note that in this paper, the surface texture of a region can only be retrieved.

**3.3.2 Hybrid Synthesis Strategy.** To generate the object based on  $q_o$ , we employ a two-tier acquisition strategy that balances quality and coverage:

**Retrieval-Based Acquisition.** Given query  $q_o$ , we first search a curated model database  $\mathcal{D}$  using a composite similarity function:

$$o^* = \arg \max_{o \in \mathcal{D}} \text{score}_{\text{ret}}(o, q_o)$$

where

$$\text{score}_{\text{ret}}(o, q_o) = \frac{\lambda_v \cdot \text{sim}_{\text{visual}}(o, q_o) + \lambda_t \cdot \text{sim}_{\text{semantic}}(o, q_o)}{\lambda_v + \lambda_t},$$

$\text{sim}_{\text{visual}}$  measures visual similarity (normalized to  $[0, 1]$ ) using CLIP embeddings [49] of rendered model views, and  $\text{sim}_{\text{semantic}}$  computes semantic similarity (normalized to  $[0, 1]$ ) between textual descriptions using Sentence-BERT [51]. The weights  $\lambda_v$  and  $\lambda_t$  are tuned empirically to balance visual fidelity and semantic accuracy.

**Generative Acquisition.** If no suitable model is found in  $\mathcal{D}$ , i.e.,  $\max_{o \in \mathcal{D}} \text{score}_{\text{ret}}(o, q_o) < \tau$  for some threshold  $\tau$ , we invoke a text-to-3D generation technique.

Any acquired object is checked by a vision language model (VLM) to ensure that it is oriented canonically. Specifically, we first rotate the object along the  $x$ -axis by  $0^\circ$ ,  $90^\circ$ ,  $180^\circ$ , and  $270^\circ$ , each time rendering the camera view. Then, we combine the renderings in a  $2 \times 2$  grid. A VLM is prompted with this combined image to determine the rotation required to put the object in upright and front-facing orientation.  $z$  and  $y$  rotations are determined in the same way.

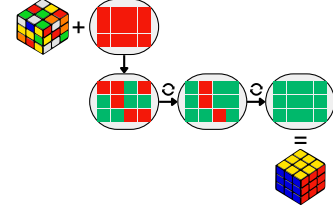


**Figure 4: Rubik Spatial Constraint Solver for spatial layout reasoning**

---

#### Algorithm 1 Rubik Spatial Constraint Solver for spatial layout reasoning

---

**Require:** Object set  $\mathcal{O}$ , constraint set  $C$ , batch size  $k$ , max iterations  $T$   
**Ensure:** Valid layout  $L^*$  satisfying all hard constraints in  $C$

- 1:  $L_0 \leftarrow \text{INITIALPLACEMENT}(\mathcal{O})$
- 2:  $L_0 \leftarrow \text{PHYSICSRELAXATION}(L_0)$
- 3: **for**  $t = 1$  to  $T$  **do**
- 4:    $\mathcal{U} \leftarrow \{c \in C : \neg \text{SATISFIED}(c, L_{t-1})\}$
- 5:   **if**  $|\mathcal{U}| = 0$  **then**
- 6:     **return**  $L_{t-1}$
- 7:   **end if**
- 8:    $\mathcal{B} \leftarrow \text{SELECTBATCH}(\mathcal{U}, k)$
- 9:    $L_t \leftarrow \text{LLMSOLVE}(L_{t-1}, \mathcal{B}, C)$
- 10:    $L_t \leftarrow \text{ENFORCEBOUNDS}(L_t)$
- 11: **end for**
- 12: **return**  $\text{BESTSOLUTION}(L_0, L_1, \dots, L_T)$

---

### 3.4 Stage III: Spatial Layout Solving

With the generated separate objects, the next step is to organize them properly in the scene. The third stage constitutes the core innovation of our approach: formulating scene layout as a constraint satisfaction problem over continuous 3D space. This principled approach provides strong guarantees about constraint satisfaction while remaining computationally tractable.

**3.4.1 Iterative Constraint Resolution Algorithm.** Our solver employs a novel iterative approach inspired by Rubik’s cube solving, where local adjustments propagate to achieve global constraint satisfaction. Algorithm 1 presents the complete procedure.

The algorithm begins with INITIALPLACEMENT (line 1), which generates a baseline layout by considering all constraints at once. PHYSICSRELAXATION (line 2) applies basic collision resolution to create a physically stable starting configuration.

The core solving loop (lines 3~10) iteratively addresses unsatisfied constraints in batches. For each batch  $\mathcal{B}$  of size  $k$ , we invoke LLMSOLVE, which leverages the spatial reasoning capabilities of LLMs to suggest object transformations. The LLM receives a structured description of the current layout, the violated constraints, and the complete constraint set, then proposes specific adjustments (translations, rotations) to resolve the violations.

**Convergence and Correctness:** The batched approach ensures stability by limiting the number of simultaneous changes, while the iterative refinement systematically reduces constraint violations. The algorithm terminates when all hard constraints are satisfied or when the maximum iteration limit is reached. In the latter case, we return the configuration with the highest constraint satisfaction rate.

### 3.5 Stage IV: Software Synthesis

The final stage combines the solved object layout with the acquired 3D models to produce an executable Unity scene file. This stage ensures that the abstract solution is materialized as a concrete software artifact suitable for immediate use in applications.

**3.5.1 Geometric Integration.** The 3D models of objects are instantiated at their solved positions and orientations, with appropriate scaling to match dimensional constraints. For the entire scene, SCENETHESIS performs several integration steps: (1) Mesh alignment, which ensures that object contact points (e.g., table legs, lamp bases) align correctly with supporting surfaces. (2) Material application, which applies specified colors, textures, and material properties with proper UV mapping. (3) Lighting configuration, which positions light sources according to solved constraints and configures parameters based on the scene atmosphere.

**3.5.2 Unity Scene Generation and Metadata Embedding.** The assembled scene is then exported as a Unity-compatible project containing: (1) **Asset files:** 3D meshes in standard formats (FBX/OBJ) with associated materials and textures. (2) **Physics components:** Collision meshes and rigidbody configurations for realistic interaction. (3) **Metadata:** Embedded SCENETHESISLANG specification enabling traceability and post-generation modification.

The generated scene is immediately usable in Unity with full physics simulation, navigation mesh generation, and interaction capabilities. The embedded metadata supports **round-trip engineering:** developers can query the scene for its generated constraints, modify the specification, and regenerate specific components without starting from scratch.

This comprehensive methodology provides a principled approach to constraint-sensitive 3D scene synthesis that addresses the fundamental limitations of existing generative methods. By decomposing the complex problem into four verifiable stages connected by a formal DSL, SCENETHESIS achieves both correctness guarantees and practical scalability while maintaining full transparency and control throughout the synthesis process.

## 4 Dataset Construction

Evaluating SCENETHESIS requires a comprehensive dataset of natural language scene descriptions paired with ground truth specifications. However, existing text-to-3D datasets either focus on single objects instead of complete 3D scenes, or don't contain queries with complicated constraints. Hence, they cannot comprehensively evaluate the effectiveness of our 3D software generation approaches. To address this problem, we developed a systematic pipeline that leverages LLMs to generate diverse indoor scene descriptions with both explicit requirements and implicit constraints, based on existing 3D scenes. Our pipeline consists of three phases, striking a balance between creative diversity and systematic coverage through structured variability.

**Phase I: Scene Structure Generation.** We define five building categories (apartment, mall, office, restaurant, school) with curated room pools (on average, each pool has 36.8 room types). For each scene, we randomly select 1–2 rooms, assign 5–15 descriptive attributes per room, and shuffle the order to prevent LLM biases.

This structured randomization ensures semantic coherence while avoiding stereotypical configurations.

For spatial connectivity, we first construct a connected graph with appropriate non-window connections to maintain semantic validity, and then probabilistically add additional connections (50% chance per room pair) for realistic multiply-connected environments. Connections receive descriptive attributes via LLM generation.

**Phase II: Content Specification.** For each room, we generate: (1) object inventories with quantity constraints (max 5 per type; 20% reduction probability, possibly down to 0), (2) concise visual descriptions for 3D retrieval/generation, (3) spatial relations driven by natural language, and (4) holistic room descriptions. The LLM synthesizes these elements into coherent natural language descriptions that SCENETHESIS must parse and realize.

**Phase III: Finalization and Validation.** Individual room descriptions and connections are integrated with building summaries, and then transformed via an LLM into a natural, conversational description that simulates real user input. This tests our system's ability to handle varied linguistic styles while extracting precise requirements. For the sake of evaluation (because some evaluation tools like CLIP [49] cannot handle input texts that are too long), we also simplify the above comprehensive and long description into one concise and short sentence using an LLM.

Our pipeline produced 50 indoor scenes with a total of 75 rooms (5 1-room and 5 2-room scenes for each building category), 2032 objects, and 1837 spatial relations. The average length of the original generated description is 508.4 words, while that of the simplified one-sentence version is 28.5 words. The dataset and the generation pipeline are released to facilitate reproducible research and domain-specific evaluation.

## 5 Experiment Design

### 5.1 Research Questions

In this study, our experiment is designed to answer the following research questions:

- **RQ1 (Stage-wise Performance):** For each methodological stage of SCENETHESIS, how effectively does the stage fulfil its designated goal? Concretely, we measure:
  - **RQ1.1:** How accurately does Stage 1 (Requirement Formalization) translate NL user queries into SCENETHESISLANG specifications while preserving user intent and injecting appropriate implicit constraints?
  - **RQ1.2:** How effectively does Stage 2 (Object Synthesis) acquire appropriate 3D models through retrieval and generation, balancing visual fidelity with semantic accuracy?
  - **RQ1.3:** How efficiently and correctly does Stage 3 (Spatial Constraint Solving) resolve complex spatial constraints?
- **RQ2 (Overall Performance):** How does SCENETHESIS compare to state-of-the-art baselines in generating complete 3D software that satisfy user queries?
- **RQ3 (User Study):** How do human evaluators perceive the 3D software generated by SCENETHESIS relative to leading baselines with respect to layout coherence, spatial realism, and overall consistency?

## 5.2 Baselines

**GPT-4o** [28], **Gemini 2.5 Pro** [10] & **DeepSeek R1** [24] (direct prompting): Directly prompt the model with the original user query and ask it to generate a JSON-formatted scene configuration (with all necessary information including the position and rotation of each object) to illustrate the end-to-end performance of LLM.

**Holodeck** [73] is also an LLM-powered module-by-module system that can generate different environments with the help of a depth-first search (DFS) solver. We again use GPT-4o, Gemini 2.5 Pro, and DeepSeek R1 to run tests on it.

## 5.3 Implementation Details of SCENETHESIS

SCENETHESIS is implemented as a modular Python framework with pluggable components for each pipeline stage.

The modular architecture of SCENETHESIS supports extensive customization for domain-specific applications. The SCENETHESIS-LANG grammar can be extended with domain-specific predicates and constraints (e.g., accessibility requirements for architectural design, safety constraints for industrial simulations). New constraint types are automatically integrated into the solving process without requiring modifications to the core algorithm. (1) The asset synthesis module supports pluggable synthesis strategies, allowing users to integrate custom model databases, proprietary generation systems, or specialized asset processing pipelines. The unified query interface ensures that new acquisition methods seamlessly integrate with existing functionality. (2) Custom constraint solvers can be developed for specialized domains that require alternative solving strategies. For example, physics-based simulation domains might benefit from continuous optimization solvers, while discrete placement problems might prefer constraint programming approaches. (3) The output generation stage supports multiple export formats and can be extended with custom drivers for specific game engines or simulation platforms. This flexibility ensures that SCENETHESIS can adapt to evolving toolchain requirements without architectural changes. Through these design principles and implementation strategies, SCENETHESIS provides a robust, scalable, and extensible foundation for constraint-sensitive 3D scene synthesis that addresses the unique requirements of SE applications while maintaining the flexibility needed for diverse use cases.

## 5.4 Experimental Setup

**5.4.1 RQ1 and RQ2.** For generating our dataset, we use deepseek-v3-0324 [42]. For running SCENETHESIS and baselines, we use gpt-4o-2024-11-20 [28], gemini-2.5-pro-preview-06-05 [10], and deepseek-r1-250528 [24]. For object canonical orientation detection and Visual Question Answering (VQA, one of our visual metrics), we use claude-3-7-sonnet-20250219 [3]. The non-repetitive use of LLMs ensures that experimental results are less likely to be biased towards a particular LLM backbone. Though, it should be noted that SCENETHESIS supports any LLM with sufficient reasoning capabilities. Also, the temperature parameter for all LLM calls is set to 0.7 (except for the use of 0 in scene type classification at Stage I, object canonical orientation detection at Stage II, and VQA).

In Stage I, we set  $v_r = v_c = 2$  for constraint validation and modification, and  $\eta = 0.03$  for wall thickness. In Stage III, we set  $k = 3$  and  $T = 5$  for the constraint solver.

Regarding our hybrid object acquisition strategy, we utilize the database curated by Holodeck [73] (which is a subset of assets from Objaverse 1.0 [12]) for retrieval-based acquisition (with  $\lambda_v$  and  $\lambda_t$  set to 100 and 1 respectively), and we choose Shap-E [30] as the underlying text-to-3D generation model for generative acquisition. As for region surface texture retrieval, we utilize another database used by Holodeck (which comes from ProcTHOR [13]). Again, because SCENETHESIS is a modular framework, any object database and generation model would work just fine.

**5.4.2 RQ3: User Study Design.** For RQ3, we conducted a user study to evaluate the perceptual quality of 3D software generated by SCENETHESIS compared to baseline approaches. We recruited 20 undergraduate or postgraduate students with backgrounds in computer science, human-computer interaction, or 3D design. All participants had at least basic familiarity with 3D environments and software evaluation.

**Study Design.** We randomly sampled 25 scenes from our evaluation dataset, ensuring balanced representation across different scene types (apartment, office, restaurant, etc.). For each scene, we give participants the top-down view of generated 3D software from three methods: (1) SCENETHESIS with Gemini-2.5-Pro backbone, (2) End-to-end LLM with Gemini-2.5-Pro, and (3) Holodeck with Gemini-2.5-Pro. This resulted in 75 total 3D scenes for evaluation.

Participants evaluated each scene along three dimensions through a web-based interface. The evaluation scores can be any float number in the range of 1-5. (1) **Layout Coherence:** "How well are objects arranged and organized in this scene?" (2) **Spatial Realism:** "How realistic are the spatial relationships between objects?" (3) **Overall Consistency:** "How well does this scene fit together as a coherent whole?"

The top-down views were presented in randomized order without method labels to prevent bias. Each participant evaluated all 75 scenes across three sessions to avoid fatigue.

## 5.5 Evaluation Metrics

We evaluate SCENETHESIS in terms of constraint resemblance, object-query coherence, solution correctness, and scene-query coherence.

**5.5.1 Stage I: Constraint Resemblance.** In SCENETHESISLANG, constraints are divided into two types: object constraints and layout constraints. To evaluate whether SCENETHESIS can generate object constraints that match those in the ground truth (i.e., our dataset), we first use Phrase-BERT [61] and Sentence-BERT [51] to compute the high-dimensional embeddings for object names and descriptions respectively. Then, we compute the dot-product (scaled to  $[0, 1]$ ) between every pair of object names as well as every pair of object descriptions. The confidence that a generated object matches a ground truth object is the harmonic mean between the corresponding "name" and "description" scaled dot-products. Next, we use the Hungarian algorithm to create a one-to-one mapping from the generated objects to the ground truth objects. Entries in this matrix that are smaller than threshold  $\tau_o$  are zeroed out. Finally, to compute the F1 score ( $\frac{2 \times \text{precision} \times \text{recall}}{\text{precision} + \text{recall}}$ , where  $\text{precision} = \frac{TP}{TP+FP}$  and  $\text{recall} = \frac{TP}{TP+FN}$ ), we define  $TP$  as the number generated objects that are mapped to one (and only one) ground truth object,  $FP$  as the number of generated objects that are not mapped to any

ground truth object, and  $FN$  as the number of ground truth objects that are not mapped to any generated object.

As for layout constraints, we first translate each generated constraint into some NL (i.e., an intuitive and human-understandable sentence). Then, we use Sentence-BERT to compute the embeddings of the translated generated constraints and ground truth NL-driven constraints. We then compute the scaled dot-product between every pair of generated and ground truth constraints, creating a confidence matrix (in some sense, a many-to-many mapping). For each entry in this matrix, if either (1) no object name from the corresponding ground truth constraint exists in the corresponding generated constraint or (2) it is smaller than a threshold  $\tau_l$ , the entry is zeroed out. Finally, to compute the F1 score, we define  $TP$  as the number of ground truth constraints that are mapped to at least one generated constraint,  $FP$  as the number of unmapped generated constraints, and  $FN$  as the number of unmapped ground truth constraints.

The overall resemblance is the harmonic mean between the two kinds of precisions, recalls, and F1 scores (with  $\tau_o = \tau_l$ ).

**5.5.2 Stage II: Object-Query Coherence.** For each acquired object, we (1) compute its smallest bounding sphere (with radius  $r$  units), (2) place a camera  $r \sin \frac{FOV}{2}$  units away from the object (where  $FOV$  (in radian) is the field of view of the camera) pointing towards the front-facing side of the object, and (3) render the camera view using Blender on a white background. We then use BLIP-2 [32] (with its ITM head) and CLIP [25, 49] to measure the coherence between the formulated object query generated by SCENETHESIS and the rendered image. To reduce bias, in addition to the object query itself, we further pass a combination of “a 3D model of” followed by the object query to the evaluation tools, and the final tool-wise score is the maximum between the two trials. The overall coherence is the arithmetic mean between the final BLIP and CLIP scores.

**5.5.3 Stage III: Solution Correctness.** We first parse each DSL-based layout constraint into an abstract syntax tree (AST). Then, for each version of solution, we count the number of satisfied constraints. The correctness of a particular version of solution is the ratio between the number of satisfied constraints and the total number of constraints (i.e., recall).

**5.5.4 Stage IV: Scene-Query Coherence.** Similar to Stage II, we place a camera at some distance away from the entire composed scene (with the ceiling removed). But this time, the camera is placed above the scene (and so the perspective is top-down). After rendering, apart from BLIP-2 and CLIP, we also use Visual Question Answering (VQA) with an LLM agent [78] to measure the coherence between the original user query (as well as a simplified one-sentence version generated by LLM) and the rendered image. Again, to reduce bias, we further pass a combination of “a top-down view of” followed by the user query to the evaluation tools. Note that objects in a target scene are acquired by setting  $\tau$  to the best value that yields the highest overall object-query coherence. This is also the metric we use to compare with the baselines.

**Table 1: Requirement formalization performance (%) across object constraints, layout constraints, and overall (harmonic mean). Best results in each metric are in bold.**

Model	Object Constraints			Layout Constraints			Overall		
	Prec.	Rec.	F1	Prec.	Rec.	F1	Prec.	Rec.	F1
<i>Threshold <math>\tau_o = \tau_l = 0.7</math></i>									
GPT-4o	<b>99.2</b>	98.0	<b>98.5</b>	<b>98.3</b>	80.3	86.4	<b>98.7</b>	88.3	92.1
Gemini-2.5-Pro	97.9	<b>98.7</b>	98.2	89.3	<b>99.9</b>	93.8	93.4	<b>99.3</b>	95.9
DeepSeek R1	99.1	95.9	96.7	97.1	97.1	<b>97.1</b>	98.1	96.5	<b>96.7</b>
<i>Threshold <math>\tau_o = \tau_l = 0.8</math></i>									
GPT-4o	<b>99.1</b>	97.9	<b>98.4</b>	<b>69.1</b>	55.4	57.7	<b>81.4</b>	70.8	72.7
Gemini-2.5-Pro	97.6	<b>98.5</b>	97.9	33.3	<b>92.7</b>	48.0	49.6	<b>95.5</b>	64.4
DeepSeek R1	99.0	95.7	96.6	62.0	82.0	<b>69.1</b>	76.3	88.3	<b>80.5</b>
<i>Threshold <math>\tau_o = \tau_l = 0.9</math></i>									
GPT-4o	<b>97.8</b>	96.6	<b>97.1</b>	<b>14.9</b>	11.4	<b>12.0</b>	<b>25.9</b>	20.5	<b>21.4</b>
Gemini-2.5-Pro	96.8	<b>97.7</b>	<b>97.1</b>	4.0	<b>18.2</b>	6.5	7.7	<b>30.7</b>	12.2
DeepSeek R1	96.8	94.0	94.7	7.4	15.6	9.8	13.7	26.8	17.7

## 6 Results and Analysis

### 6.1 RQ1: Stage-wise Performance Analysis

To evaluate the effectiveness of SCENETHESIS’s modular pipeline, we examine each stage independently to understand its contribution to the overall system performance. We investigate how each stage fulfills its designated goal through comprehensive metrics that capture both quantitative performance and qualitative correctness.

**6.1.1 RQ1.1: Requirement Formalization Accuracy.** We first evaluate how accurately Stage I translates natural language queries into SCENETHESISLANG specifications while preserving user intent and injecting appropriate implicit constraints. We measure performance separately for object constraints and layout constraints, as they represent fundamentally different challenges in formalization.

Tables 1 present the formalization performance for object and layout constraints, respectively. For object constraints, all models achieve consistently high performance ( $F1 > 0.94$ ) even at the strictest threshold ( $\tau_o = 0.9$ ), demonstrating the robustness of our formalization approach for object identification and description. GPT-4o exhibits the best balance between precision and recall, maintaining over 97% precision across all thresholds.

However, layout constraint formalization presents a more significant challenge. Performance degrades substantially as the threshold increases, with F1 scores dropping from above 0.86 at  $\tau_l = 0.7$  to below 0.13 at  $\tau_l = 0.9$  for all models. This degradation reveals the inherent difficulty in precisely capturing spatial relationships from natural language—while models can identify the general intent of spatial constraints, exact formalization remains challenging. R1 demonstrates the most robust performance, achieving the highest F1 score (0.971) at the standard threshold.

Table 1 shows the overall formalization performance. At the standard threshold ( $\tau = 0.7$ ), all models achieve strong performance with F1 scores above 0.92, validating our requirement formalization approach. R1 achieves the best overall performance ( $F1 = 0.967$ ), demonstrating superior capability in balancing object and layout constraint formalization.

**6.1.2 RQ1.2: Object Synthesis Effectiveness.** We evaluate how effectively Stage II acquires appropriate 3D models through our hybrid retrieval-generation strategy.

**Table 2: Object synthesis performance (%) comparing pure retrieval, pure generation, and our hybrid approach (R+G). Scores represent object-query coherence.**

Method	BLIP-2	CLIP	Mean
Retrieval only ( $\tau = 0.0$ )	51.2	27.1	39.1
Generation only ( $\tau = 1.0$ )	42.2	25.9	34.1
<b>R+G (<math>\tau = 0.652</math>)</b>	<b>51.6</b>	<b>27.1</b>	<b>39.3</b>

**Table 3: Spatial constraint solving performance across iterations. Scores (%) represent the ratio of satisfied constraints (solution correctness).**

Model	Iter 0	Iter 1	Iter 2	Iter 3	Iter 4	Iter 5
GPT-4o	47.1	60.4	63.2	65.6	67.3	<b>68.3</b>
Gemini-2.5-Pro	74.1	91.1	92.5	<b>93.8</b>	93.5	93.4
DeepSeek R1	47.8	87.6	90.6	91.7	92.9	<b>93.0</b>

Table 2 presents the object synthesis results. Our hybrid approach (R+G) achieves the best performance across both metrics, with a mean coherence score of 39.3. The results validate our design decision to combine retrieval and generation: retrieval provides high-quality models when available in the database (BLIP score of 51.2), while generation ensures coverage for novel objects. The optimal threshold  $\tau = 0.652$  effectively balances between leveraging existing high-quality assets and generating new models when necessary.

Notably, pure retrieval outperforms pure generation by 5.0 points on average, confirming that curated 3D model databases contain higher-quality assets than current text-to-3D generation methods can produce. However, the retrieval-only approach suffers from limited coverage—approximately 23% of queries fail to find suitable matches, necessitating our hybrid strategy.

**6.1.3 RQ1.3: Spatial Constraint Solving Efficiency.** We evaluate the efficiency and correctness of Stage III in resolving complex spatial constraints through our iterative Rubik solver.

Table 3 demonstrates the iterative improvement of our Rubik solver. All models show substantial improvement from the initial placement (Iteration 0) to the final solution, with Gemini-2.5-Pro achieving the highest constraint satisfaction rate of 93.8% at convergence. The rapid improvement in early iterations (e.g., Gemini-2.5-Pro jumping from 74.1% to 91.1% in the first iteration) validates our local-to-global refinement strategy. The results reveal interesting patterns: while GPT-4o starts with the lowest initial placement quality (47.1%), it shows steady improvement across iterations. In contrast, Gemini-2.5-Pro begins with superior initial placements (74.1%) and quickly converges to near-optimal solutions. R1 demonstrates the most consistent improvement trajectory, ultimately achieving 93.0% constraint satisfaction.

**6.1.4 Summary of RQ1 Findings.** Our stage-wise evaluation demonstrates that SCENETHESIS’s modular pipeline effectively addresses the key challenges in 3D software synthesis: **Stage I** successfully formalizes natural language requirements with high accuracy for object constraints ( $F1 > 0.94$ ) and reasonable performance for layout constraints at standard thresholds, with R1 achieving the best overall balance. **Stage II**’s hybrid retrieval-generation strategy outperforms either approach alone, effectively balancing quality and coverage for 3D model acquisition. **Stage III**’s iterative constraint solver achieves over 93% constraint satisfaction within 5 iterations,

**Table 4: Overall performance (%) comparison against baselines. Best results for each metric are in **bold**, second-best are underlined. “O” → “Original”, “S” → “Sentence”.**

Method	LLM Backbone	BLIP-2		CLIP		VQA	
		O	S	O	S	O	S
SCENETHESIS (Ours)	GPT-4o	71.3	69.9	25.6	<u>25.5</u>	28.3	44.8
	Gemini 2.5 Pro	<b>74.3</b>	<b>75.1</b>	26.1	25.5	<u>29.5</u>	<u>47.9</u>
	DeepSeek R1	<u>72.5</u>	<u>74.7</u>	<b>26.2</b>	<b>25.8</b>	<b>29.8</b>	<b>48.6</b>
End-to-end LLM	GPT-4o	61.9	60.0	24.7	24.0	15.1	28.6
	Gemini 2.5 Pro	71.6	73.2	25.6	25.3	27.1	41.1
	DeepSeek R1	72.1	69.9	24.9	24.7	23.9	38.9
Holodeck [73]	GPT-4o	60.0	62.2	23.7	22.5	24.7	37.7
	Gemini 2.5 Pro	67.0	66.5	24.2	23.5	26.0	42.1
	DeepSeek R1	53.1	52.3	23.6	22.9	19.8	31.8

demonstrating both efficiency and effectiveness in handling complex spatial relationships. These results validate our decomposition approach: by breaking down the complex 3D synthesis problem into specialized stages, we achieve both high performance and maintainability, addressing the fundamental software engineering challenges identified in our introduction.

## 6.2 RQ2: Overall Performance

To evaluate the overall performance of SCENETHESIS in generating complete 3D software that satisfies user queries, we compare our approach against state-of-the-art baselines across multiple visual coherence metrics. Table 4 presents the comprehensive evaluation results.

**Visual Coherence Performance.** Our results demonstrate that SCENETHESIS consistently outperforms baseline approaches across all evaluation metrics. For BLIP-2 scores, which measure image-text alignment, SCENETHESIS achieves an average improvement of 4.8% over the best-performing baseline (End-to-end LLM with Gemini 2.5 Pro). The improvement is even more pronounced when using sentence-level queries, where our method with DeepSeek R1 achieves 74.7%, indicating better understanding of user intent.

**Semantic Understanding.** The VQA metrics reveal the most significant advantages of our approach. SCENETHESIS with DeepSeek R1 achieves 29.8% on original queries and 48.6% on sentence-level queries, representing improvements of 10.0% and 18.3% respectively over the best baseline results. This substantial improvement demonstrates that our structured approach, which decomposes scene generation into well-defined stages with explicit constraint handling, produces 3D software that better aligns with user specifications.

**Impact of LLM Backend.** Interestingly, while all three LLM backends show strong performance with our method, DeepSeek R1 exhibits the most consistent results across all metrics when integrated with SCENETHESIS. In contrast, the same model shows significant performance degradation when used with Holodeck (averaging only 53.1% on BLIP-2), suggesting that our modular architecture better leverages the reasoning capabilities of modern LLMs.

**Robustness Across Query Types.** The relatively stable performance between original and sentence-level queries (with differences typically under 3%) indicates that SCENETHESIS robustly handles both detailed specifications and simplified descriptions.

**Table 5: User study results (mean scores  $\pm$  std. dev.) comparing perceived quality of 3D scenes. All scores on 1-5 scale, higher is better. Best results in bold.**

Method	Layout Coherence	Spatial Realism	Overall Consistency
SCENETHESIS (Ours)	<b>4.12</b>	<b>3.89</b>	<b>4.05</b>
End-to-end LLM	3.45	3.21	3.38
Holodeck	3.68	3.42	3.61

This is particularly important for practical applications where users may provide varying levels of detail in their requirements.

The consistent superiority of SCENETHESIS across diverse evaluation metrics validates our hypothesis that treating 3D software synthesis as a structured SE problem (with formal specifications, verifiable constraints, and modular components) leads to more reliable and higher-quality outputs compared to monolithic generation approaches.

### 6.3 RQ3: User Study

Table 5 presents the user study results. SCENETHESIS consistently outperforms both baselines across all evaluation dimensions, with statistically significant improvements.

For layout coherence, SCENETHESIS achieves a mean score of 4.12, representing a 19.4% improvement over the best baseline (Holodeck). Participants noted that objects generated by our method exhibited more logical groupings and functional arrangements. The modular synthesis pipeline with explicit constraint handling produces layouts that better reflect real-world organizational principles.

Spatial realism scores show similar advantages, with SCENETHESIS achieving 3.89 compared to 3.42 for Holodeck. The iterative constraint solver’s ability to handle continuous spatial relationships results in more natural object placements, avoiding the categorical limitations of scene graph-based approaches.

Overall consistency ratings confirm that our decomposition approach produces more coherent 3D software. The formal SCENETHESISLANG specifications ensure that all scene elements work together harmoniously, while baseline methods often produce locally reasonable but globally inconsistent arrangements.

## 7 Threats to Validity

**Internal Validity.** Our constraint solver employs an iterative LLM-based approach that may not guarantee convergence for all constraint sets. The batched constraint resolution process could potentially introduce order dependencies that affect the quality of the solution. Additionally, the physics-based relaxation step may modify object placements in ways that violate previously satisfied constraints, though our evaluation suggests that this occurs infrequently in practice.

**External Validity.** Our evaluation focuses exclusively on indoor scene generation, limiting generalizability to outdoor environments or specialized domains (e.g., underwater scenes, space environments). The dataset generation process may not fully capture the complexity and diversity of real-world user requirements. Furthermore, our constraint patterns are primarily derived from residential

and commercial indoor spaces, potentially limiting applicability to industrial or artistic 3D environments.

**Construct Validity.** The evaluation metrics for constraint satisfaction rely on automated verification that may not capture subtle semantic violations perceptible to human observers. Our scene-prompt coherence metric depends on embedding similarity, which may not fully reflect human perception of scene quality. The visual quality assessment is limited to programmatic metrics rather than comprehensive human evaluation studies. To mitigate this threat, we conduct a user study to evaluate from human side.

## 8 Related Work

### 8.1 2D UI Code Generation

The automated generation of UI code from visual designs has emerged as an important research area in software engineering, driven by the need to bridge the gap between design and development workflows. Recent advances in multimodal large language models (LLMs) have shown promising capabilities in automatically generating UI code from visual designs. However, early experiments revealed critical limitations: GPT-4o exhibits omission, distortion, and misarrangement of elements when generating code directly from screenshots [58].

To address these challenges, several decomposition-based approaches have emerged. DCGen [58] adopts a divide-and-conquer strategy, segmenting screenshots into manageable regions before code generation, achieving up to 15% improvement in visual similarity. UICopilot [23] introduces hierarchical generation, first producing coarse HTML structure then fine-grained implementations. DeclarUI [80] combines computer vision with iterative compiler-driven optimization, achieving 96.8% page transition coverage on React Native applications.

Comprehensive benchmarks have been established to evaluate these systems. Design2Code [54] provides 484 real-world webpages with automatic metrics for code quality and visual fidelity. DesignBench [66] extends evaluation to multiple frameworks (React, Vue, Angular) across generation, editing, and repair tasks. WebCode2M [22] contributes a large-scale dataset of 2.56 million webpage instances, enabling more robust model training.

Recent work has explored layout-aware generation to improve structural accuracy. LayoutCoder [65] leverages explicit UI layout information through element relation construction, improving BLEU scores by 10.14% over baselines. Despite these advances, current methods still struggle with complex layouts, framework-specific patterns, and interactive behaviors, limiting their practical deployment in production environments.

### 8.2 3D Software Generation

The rapid expansion of 3D software systems, from flat 3D to stereoscopic 3D [34, 35, 37–40], demands automated approaches for automated generation.

Early probabilistic approaches [6, 7, 18, 29, 44, 53, 77] model object distributions in training scenes to enable sampling during inference. For instance, SceneSeer [7] parses text prompts using fixed grammars and computes probable scene templates. However, these

methods suffer from limited object class diversity due to their reliance on predefined categorical distributions, severely constraining the variety of testable scenarios.

The predominant paradigm employs deep learning architectures to learn scene representations. Methods utilizing CNNs [52, 59, 60, 70], encoder-decoders [9, 14, 21, 33, 64, 67, 68], GANs [4, 36], transformers [43, 45, 48, 62, 63, 74, 79], and diffusion models [41, 55, 71, 75, 76, 81] have demonstrated varying degrees of success. These approaches typically learn from datasets like 3D-FRONT [17] and can be conditioned on diverse inputs, ATISS [48] accepts floor layouts while InstructScene [41] processes NL for multiple scene manipulation tasks.

View-based methods [8, 11, 27, 46, 69] reconstruct 3D environments from RGB images but require physical scenes as input, contradicting the goal of automated synthesis for testing novel scenarios. Procedural generation [13, 50] employs algorithmic rules to create environments efficiently but lacks the flexibility needed for edge-case generation in software testing contexts.

Recent LLM-based approaches [2, 5, 15, 19, 20, 47, 72, 73] leverage large language models to guide scene generation. Holodeck [73], for example, uses GPT-4 to generate floor plans, object attributes, and spatial constraints before employing search-based constraint solving. While promising, these methods still inherit the limitations of scene graph representations when formalizing spatial relationships.

While these aforementioned recent advances have produced numerous approaches to automated scene generation, fundamental limitations in controllability, expressiveness, and verifiability continue to impede their adoption in SE contexts.

## 9 Conclusion

In this paper, we presented SCENETHESIS, a novel approach to 3D software synthesis that decomposes the problem into four verifiable stages connected by SCENETHESISLANG, a formal intermediate representation. Our evaluation demonstrates that SCENETHESIS achieves over 80% requirement capture accuracy, satisfies 90%+ of constraints, and improves visual quality by 42.8% over state-of-the-art methods. By applying SE principles to 3D scene generation, we enable the fine-grained control, verifiability, and maintainability required for practical deployment in safety-critical domains.

## References

- [1] 2025. How Big is the 3D Gaming Market | Trends & Forecast 2025. <https://www.6wresearch.com/market-takeaways-view/how-big-is-the-3d-gaming-market>.
- [2] Rio Aguiña-Kang, Maxim Gumin, Do Heon Han, Stewart Morris, Seung Jean Yoo, Aditya Ganesan, R Kenny Jones, QiuHong Anna Wei, Kailiang Fu, and Daniel Ritchie. 2024. Open-Universe Indoor Scene Generation using LLM Program Synthesis and Uncurated Object Databases. *arXiv preprint arXiv:2403.09675* (2024).
- [3] Anthropic. 2025. Claude 3.7 Sonnet and Claude Code. <https://www.anthropic.com/news/claude-3-7-sonnet>.
- [4] Sherwin Bahmani, Jeong Joon Park, Despoina Paschalidou, Kingguang Yan, Gordon Wetzstein, Leonidas Guibas, and Andrea Tagliasacchi. 2023. Cc3d: Layout-conditioned generation of compositional 3d scenes. In *ICCV*. 7171–7181.
- [5] Ata Çelen, Guo Han, Konrad Schindler, Luc Van Gool, Iro Armeni, Anton Obukhov, and Xi Wang. 2024. I-design: Personalized llm interior designer. *arXiv preprint arXiv:2404.02838* (2024).
- [6] Angel Chang, Will Monroe, Manolis Savva, Christopher Potts, and Christopher D. Manning. 2015. Text to 3D Scene Generation with Rich Lexical Grounding. In *ACL-IJCNLP*, Chengqing Zong and Michael Strube (Eds.). Association for Computational Linguistics, Beijing, China, 53–62. <https://doi.org/10.3115/v1/P15-1006>
- [7] Angel X Chang, Mihail Eric, Manolis Savva, and Christopher D Manning. 2017. SceneSeer: 3D scene design with natural language. *arXiv preprint arXiv:1703.00050* (2017).
- [8] Jit Chatterjee and Maria Torres Vega. 2024. 3D-Scene-Former: 3D scene generation from a single RGB image using Transformers. *The Visual Computer* (07 2024), 1–15. <https://doi.org/10.1007/s00371-024-03573-2>
- [9] Aditya Chattopadhyay, Xi Zhang, David Paul Wipf, Himanshu Arora, and René Vidal. 2023. Learning Graph Variational Autoencoders with Constraints and Structured Priors for Conditional Indoor 3D Scene Generation. In *WACV*. 785–794. <https://doi.org/10.1109/WACV56688.2023.00085>
- [10] Gheorghe Comanici, Eric Bieber, Mike Schaeckermann, Ice Pasupat, Noveen Sachdeva, Inderjit Dhillon, Marcel Blistein, Ori Ram, Dan Zhang, Evan Rosen, et al. 2025. Gemini 2.5: Pushing the Frontier with Advanced Reasoning, Multimodality, Long Context, and Next Generation Agentic Capabilities. *arXiv preprint arXiv:2507.06261* (2025).
- [11] Tianyuan Dai, Josiah Wong, Yunfan Jiang, Chen Wang, Cem Gokmen, Ruohan Zhang, Jiajun Wu, and Li Fei-Fei. 2024. Acdd: Automated creation of digital cousins for robust policy learning. *arXiv preprint arXiv:2410.07408* (2024).
- [12] Matt Deitke, Dustin Schwenk, Jordi Salvador, Luca Weihs, Oscar Michel, Eli VanderBilt, Ludwig Schmidt, Kiana Ehsani, Aniruddha Kembhavi, and Ali Farhadi. 2023. Objaverse: A universe of annotated 3d objects. In *CVPR*. 13142–13153.
- [13] Matt Deitke, Eli VanderBilt, Alvaro Herrasti, Luca Weihs, Kiana Ehsani, Jordi Salvador, Winson Han, Eric Kolbe, Aniruddha Kembhavi, and Roozbeh Motlaghi. 2022. ProcTHOR: Large-Scale Embodied AI Using Procedural Generation. *NeurIPS* 35 (2022), 5982–5994.
- [14] Helisa Dharmo, Fabian Manhardt, Nassir Navab, and Federico Tombari. 2021. Graph-to-3d: End-to-end generation and manipulation of 3d scenes using scene graphs. In *ICCV*. 16352–16361.
- [15] Weixi Feng, Wanrong Zhu, Tsu-jui Fu, Varun Jampani, Arjun Akula, Xuehai He, Sugato Basu, Xin Eric Wang, and William Yang Wang. 2024. Layoutgpt: Compositional visual planning and generation with large language models. *NeurIPS* 36 (2024).
- [16] James D. Foley, Steven K. Van Dam, and Kurt Akeley. 2013. *Computer graphics: principles and practice* (3rd ed.). Addison-Wesley Professional.
- [17] Huan Fu, Bowen Cai, Lin Gao, Ling-Xiao Zhang, Jiaming Wang, Cao Li, Qixun Zeng, Chengyue Sun, Rongfei Jia, Binjiang Zhao, et al. 2021. 3d-front: 3d furnished rooms with layouts and semantics. In *ICCV*. 10933–10942.
- [18] Qiang Fu, Xiaowu Chen, Xiaotian Wang, Sijia Wen, Bin Zhou, and Hongbo Fu. 2017. Adaptive synthesis of indoor scenes via activity-associated object relation graphs. *ACM Trans. Graph.* 36, 6, Article 201 (Nov. 2017), 13 pages. <https://doi.org/10.1145/3130800.3130805>
- [19] Rao Fu, Zehao Wen, Zichen Liu, and Srinath Sridhar. 2025. Anyhome: Open-vocabulary generation of structured and textured 3d homes. In *ECCV*. Springer, 52–70.
- [20] Gege Gao, Weiyang Liu, Anpei Chen, Andreas Geiger, and Bernhard Schölkopf. 2024. Graphdreamer: Compositional 3d scene synthesis from scene graphs. In *CVPR*. 21295–21304.
- [21] Lin Gao, Jia-Mu Sun, Kaichun Mo, Yu-Kun Lai, Leonidas J Guibas, and Jie Yang. 2023. Scenehgn: Hierarchical graph networks for 3d indoor scene generation with fine-grained geometry. *IEEE Transactions on Pattern Analysis and Machine Intelligence* 45, 7 (2023), 8902–8919.
- [22] Yi Gui, Zhen Li, Yao Wan, Yemin Shi, Hongyu Zhang, Bohua Chen, Yi Su, Dongping Chen, Siyuan Wu, Xing Zhou, et al. 2025. Webcode2m: A real-world dataset for code generation from webpage designs. In *WWW*. 1834–1845.
- [23] Yi Gui, Yao Wan, Zhen Li, Zhongyi Zhang, Dongping Chen, Hongyu Zhang, Yi Su, Bohua Chen, Xing Zhou, Wenbin Jiang, et al. 2025. UICoPilot: Automating UI synthesis via hierarchical code generation from webpage designs. In *WWW*. 1846–1855.
- [24] Daya Guo, Dejian Yang, Haowei Zhang, Junxiao Song, Ruoyu Zhang, Runxin Xu, Qihao Zhu, Shirong Ma, Peiyi Wang, Xiao Bi, et al. 2025. Deepseek-r1: Incentivizing reasoning capability in llms via reinforcement learning. *arXiv preprint arXiv:2501.12948* (2025).
- [25] Jack Hessel, Ari Holtzman, Maxwell Forbes, Ronan Le Bras, and Yejin Choi. 2021. Clipscore: A reference-free evaluation metric for image captioning. *arXiv preprint arXiv:2104.08718* (2021).
- [26] Lukas Höllein, Ang Cao, Andrew Owens, Justin Johnson, and Matthias Nießner. 2023. Text2room: Extracting textured 3d meshes from 2d text-to-image models. In *ICCV*. 7909–7920.
- [27] Siyuan Huang, Siyuan Qi, Yixin Zhu, Yinxue Xiao, Yuanlu Xu, and Song-Chun Zhu. 2018. Holistic 3d scene parsing and reconstruction from a single rgb image. In *ECCV*. 187–203.
- [28] Aaron Hurst, Adam Lerer, Adam P Goucher, Adam Perelman, Aditya Ramesh, Aidan Clark, AJ Ostrow, Akila Welihinda, Alan Hayes, Alec Radford, et al. 2024. Gpt-4o system card. *arXiv preprint arXiv:2410.21276* (2024).
- [29] Chenfanfu Jiang, Siyuan Qi, Yixin Zhu, Siyuan Huang, Jenny Lin, Lap-Fai Yu, Demetri Terzopoulos, and Song-Chun Zhu. 2018. Configurable 3d scene synthesis and 2d image rendering with per-pixel ground truth using stochastic grammars. *International Journal of Computer Vision* 126 (2018), 920–941.

- [30] Heewoo Jun and Alex Nichol. 2023. Shap-e: Generating conditional 3d implicit functions. *arXiv preprint arXiv:2305.02463* (2023).
- [31] Haoran Li, Haolin Shi, Wenli Zhang, Wenjun Wu, Yong Liao, Lin Wang, Likhang Lee, and Pengyuan Zhou. 2024. DreamScene: 3D Gaussian-based Text-to-3D Scene Generation via Formation Pattern Sampling. *arXiv preprint arXiv:2404.03575* (2024).
- [32] Junnan Li, Dongxu Li, Silvio Savarese, and Steven Hoi. 2023. Blip-2: Bootstrapping language-image pre-training with frozen image encoders and large language models. In *PLMR*. 19730–19742.
- [33] Manyi Li, Akshay Gadi Patil, Kai Xu, Siddhartha Chaudhuri, Owais Khan, Ariel Shamir, Changhe Tu, Baoquan Chen, Daniel Cohen-Or, and Hao Zhang. 2019. Grains: Generative recursive autoencoders for indoor scenes. *ACM Transactions on Graphics (TOG)* 38, 2 (2019), 1–16.
- [34] Shuqing Li, Cuiyun Gao, Jianping Zhang, Yujia Zhang, Yepang Liu, Jiazhen Gu, Yun Peng, and Michael R Lyu. 2024. Less cybersickness, please: Demystifying and detecting stereoscopic visual inconsistencies in virtual reality apps. *Proceedings of the ACM on Software Engineering* 1, FSE (2024), 2167–2189.
- [35] Shuqing Li, Binchang Li, Yepang Liu, Cuiyun Gao, Jianping Zhang, Shing-Chi Cheung, and Michael R Lyu. 2024. Grounded gui understanding for vision based spatial intelligent agent: Exemplified by virtual reality apps. *arXiv preprint arXiv:2409.10811* (2024).
- [36] Shuai Li and Hongjun Li. 2023. Deep Generative Modeling Based on VAE-GAN for 3D Indoor Scene Synthesis. *International Journal of Computer Games Technology* 2023, 1 (2023), 3368647. <https://doi.org/10.1155/2023/3368647> arXiv:<https://onlinelibrary.wiley.com/doi/pdf/10.1155/2023/3368647>
- [37] Shuqing Li, Lili Wei, Yepang Liu, Cuiyun Gao, Shing-Chi Cheung, and Michael R Lyu. 2023. Towards modeling software quality of virtual reality applications from users' perspectives. *arXiv preprint arXiv:2308.06783* (2023).
- [38] Shuqing Li, Yechang Wu, Yi Liu, Dinghua Wang, Ming Wen, Yida Tao, Yulei Sui, and Yepang Liu. 2020. An exploratory study of bugs in extended reality applications on the web. In *ISSRE*. IEEE, 172–183.
- [39] Shuqing Li, Chenran Zhang, Cuiyun Gao, and Michael R Lyu. 2024. XRZoo: A Large-Scale and Versatile Dataset of Extended Reality (XR) Applications. *arXiv preprint arXiv:2412.06759* (2024).
- [40] Shuqing Li, Qisheng Zheng, Cuiyun Gao, Jia Feng, and Michael R Lyu. 2025. Extended Reality Cybersickness Assessment via User Review Analysis. *Proceedings of the ACM on Software Engineering* 2, ISSTA (2025), 1303–1325.
- [41] Chenguo Lin and Yadong Mu. 2024. InstructScene: Instruction-Driven 3D Indoor Scene Synthesis with Semantic Graph Prior. In *ICLR*.
- [42] Aixin Liu, Bei Feng, Bing Xue, Bingxuan Wang, Bochao Wu, Chengda Lu, Chenggang Zhao, Chengqi Deng, Chenyu Zhang, Chong Ruan, et al. 2024. Deepseek-v3 technical report. *arXiv preprint arXiv:2412.19437* (2024).
- [43] Jingyu Liu, Wenhan Xiong, Ian Jones, Yixin Nie, Anchit Gupta, and Barlas Öğuz. 2023. Clip-layout: Style-consistent indoor scene synthesis with semantic furniture embedding. *arXiv preprint arXiv:2303.03565* (2023).
- [44] Rui Ma, Akshay Gadi Patil, Matthew Fisher, Manyi Li, Sören Pirk, Binh-Son Hua, Sai-Kit Yeung, Xin Tong, Leonidas Guibas, and Hao Zhang. 2018. Language-driven synthesis of 3D scenes from scene databases. *ACM Trans. Graph.* 37, 6, Article 212 (Dec. 2018), 16 pages. <https://doi.org/10.1145/3272127.3275035>
- [45] Yinyu Nie, Angela Dai, Xiaoguang Han, and Matthias Nießner. 2023. Learning 3d scene priors with 2d supervision. In *CVPR*. 792–802.
- [46] Yinyu Nie, Xiaoguang Han, Shihui Guo, Yujian Zheng, Jian Chang, and Jian Jun Zhang. 2020. Total3dunderstanding: Joint layout, object pose and mesh reconstruction for indoor scenes from a single image. In *CVPR*. 55–64.
- [47] Başak Melis Öcal, Maxim Tatarchenko, Sezer Karaoglu, and Theo Gevers. 2024. SceneTeller: Language-to-3D Scene Generation. *arXiv preprint arXiv:2407.20727* (2024).
- [48] Despoina Paschalidou, Amlan Kar, Maria Shugrina, Karsten Kreis, Andreas Geiger, and Sanja Fidler. 2021. Atiss: Autoregressive transformers for indoor scene synthesis. *NeurIPS* 34 (2021), 12013–12026.
- [49] Alec Radford, Jong Wook Kim, Chris Hallacy, Aditya Ramesh, Gabriel Goh, Sandhini Agarwal, Girish Sastry, Amanda Askell, Pamela Mishkin, Jack Clark, et al. 2021. Learning transferable visual models from natural language supervision. In *PLMR*. 8748–8763.
- [50] Alexander Raistrick, Lahav Lipson, Zeyu Ma, Lingjie Mei, Mingzhe Wang, Yiming Zuo, Karhan Kayan, Hongyu Wen, Beining Han, Yihan Wang, Alejandro Newell, Hei Law, Ankit Goyal, Kaiyu Yang, and Jia Deng. 2023. Infinite Photorealistic Worlds Using Procedural Generation. In *CVPR*. 12630–12641.
- [51] Nils Reimers and Iryna Gurevych. 2019. Sentence-BERT: Sentence Embeddings using Siamese BERT-Networks. In *EMNLP*. Association for Computational Linguistics. <http://arxiv.org/abs/1908.10084>
- [52] Daniel Ritchie, Kai Wang, and Yu-an Lin. 2019. Fast and flexible indoor scene synthesis via deep convolutional generative models. In *CVPR*. 6182–6190.
- [53] Manolis Savva, Angel X Chang, and Maneesh Agrawala. 2017. Scenesuggest: Context-driven 3d scene design. *arXiv preprint arXiv:1703.00061* (2017).
- [54] Chenglei Si, Yanzhe Zhang, Ryan Li, Zhengyuan Yang, Ruibo Liu, and Diyi Yang. 2024. Design2code: Benchmarking multimodal code generation for automated front-end engineering. *arXiv preprint arXiv:2403.03163* (2024).
- [55] Jiapeng Tang, Yinyu Nie, Lev Markhasin, Angela Dai, Justus Thies, and Matthias Nießner. 2024. Diffuscene: Denoising diffusion models for generative indoor scene synthesis. In *CVPR*.
- [56] Unity Technologies. 2025. Unity 6.1 User Manual. <https://docs.unity3d.com/6000.1/Documentation/Manual/UnityManual.html>
- [57] Charles P Thacker, EM MacCreight, and Butler W Lampson. 1979. *Alto: A personal computer*. Xerox, Palo Alto Research Center Palo Alto.
- [58] Yuxuan Wan, Chaozheng Wang, Yi Dong, Wenxuan Wang, Shuqing Li, Yintong Huo, and Michael Lyu. 2025. Divide-and-Conquer: Generating UI Code from Screenshots. *PACMSE* 2, FSE (2025), 2099–2122.
- [59] Kai Wang, Yu-An Lin, Ben Weissmann, Manolis Savva, Angel X. Chang, and Daniel Ritchie. 2019. PlanIT: planning and instantiating indoor scenes with relation graph and spatial prior networks. *ACM Trans. Graph.* 38, 4, Article 132 (July 2019), 15 pages. <https://doi.org/10.1145/3306346.3322941>
- [60] Kai Wang, Manolis Savva, Angel X Chang, and Daniel Ritchie. 2018. Deep convolutional priors for indoor scene synthesis. *ACM Transactions on Graphics (TOG)* 37, 4 (2018), 70.
- [61] Shufan Wang, Laure Thompson, and Mohit Iyyer. 2021. Phrase-BERT: Improved phrase embeddings from BERT with an application to corpus exploration. *arXiv preprint arXiv:2109.06304* (2021).
- [62] Xinpeng Wang, Chandan Yeshwanth, and Matthias Nießner. 2021. Sceneformer: Indoor scene generation with transformers. In *3DV*. IEEE, 106–115.
- [63] Qihong Anna Wei, Sijie Ding, Jeong Joon Park, Rahul Sajjani, Adrien Poulenard, Srinath Sridhar, and Leonidas Guibas. 2023. Lego-net: Learning regular rearrangements of objects in rooms. In *CVPR*. 19037–19047.
- [64] Yao Wei, Martin Renqiang Min, George Vosselman, Li Erran Li, and Michael Ying Yang. 2024. Planner3D: LLM-enhanced graph prior meets 3D indoor scene explicit regularization. *arXiv preprint arXiv:2403.12848* (2024).
- [65] Fan Wu, Cuiyun Gao, Shuqing Li, Xin-Cheng Wen, and Qing Liao. 2025. MLLM-Based UI2Code Automation Guided by UI Layout Information. *PACMSE* 2, ISSTA (2025), 1123–1145.
- [66] Jingyu Xiao, Ming Wang, Man Ho Lam, Yuxuan Wan, Junliang Liu, Yintong Huo, and Michael R Lyu. 2025. Designbench: A comprehensive benchmark for mllm-based front-end code generation. *arXiv preprint arXiv:2506.06251* (2025).
- [67] Rui Xu, Le Hui, Yuehui Han, Jianjun Qian, and Jin Xie. 2023. Scene Graph Masked Variational Autoencoders for 3D Scene Generation. In *ACM Multimedia* (Ottawa ON, Canada) (*MM '23*). Association for Computing Machinery, New York, NY, USA, 5725–5733. <https://doi.org/10.1145/3581783.3612262>
- [68] Haitao Yang, Zaiwei Zhang, Siming Yan, Haibin Huang, Chongyang Ma, Yi Zheng, Chandrajit Bajaj, and Qixing Huang. 2021. Scene synthesis via uncertainty-driven attribute synchronization. In *ICCV*. 5630–5640.
- [69] Ming-Jia Yang, Yu-Xiao Guo, Bin Zhou, and Xin Tong. 2021. Indoor scene generation from a collection of semantic-segmented depth images. In *ICCV*. 15203–15212.
- [70] Xinyan Yang, Fei Hu, Long Ye, Zhiming Chang, and Jiyin Li. 2022. A system of configurable 3D indoor scene synthesis via semantic relation learning. *Displays* 74 (2022), 102168. <https://doi.org/10.1016/j.displa.2022.102168>
- [71] Yandan Yang, Baoxiong Jia, Peiyuan Zhi, and Siyuan Huang. 2024. Physcene: Physically interactable 3d scene synthesis for embodied ai. In *CVPR*. 16262–16272.
- [72] Yixuan Yang, Junru Lu, Zixiang Zhao, Zhen Luo, James JQ Yu, Victor Sanchez, and Feng Zheng. 2024. LLplace: The 3D Indoor Scene Layout Generation and Editing via Large Language Model. *arXiv preprint arXiv:2406.03866* (2024).
- [73] Yue Yang, Fan-Yun Sun, Luca Weihs, Eli VanderBilt, Alvaro Herrasti, Winsong Han, Jiajun Wu, Nick Haber, Ranjay Krishna, Lingjie Liu, et al. 2024. Holodeck: Language guided generation of 3d embodied ai environments. In *CVPR*. 16227–16237.
- [74] Zhaoda Ye, Yang Liu, and Yuxin Peng. 2024. MAAN: Memory-Augmented Autoregressive Network for Text-driven 3D Indoor Scene Generation. *IEEE Transactions on Multimedia* (2024), 1–14. <https://doi.org/10.1109/TMM.2024.3443657>
- [75] Guangyao Zhai, Evin Pinar Örnek, Dave Zhenyu Chen, Ruotong Liao, Yan Di, Nassir Navab, Federico Tombari, and Benjamin Busam. 2025. Echoscene: Indoor scene generation via information echo over scene graph diffusion. In *ECCV*. Springer, 167–184.
- [76] Guangyao Zhai, Evin Pinar Örnek, Shun-Cheng Wu, Yan Di, Federico Tombari, Nassir Navab, and Benjamin Busam. 2024. Commonsences: Generating commonsense 3d indoor scenes with scene graphs. *NeurIPS* 36 (2024).
- [77] Song-Hai Zhang, Shao-Kui Zhang, Wei-Yu Xie, Cheng-Yang Luo, Yong-Liang Yang, and Hongbo Fu. 2022. Fast 3D Indoor Scene Synthesis by Learning Spatial Relation Priors of Objects. *IEEE Transactions on Visualization and Computer Graphics* 28, 9 (2022), 3082–3092. <https://doi.org/10.1109/TVCG.2021.3050143>
- [78] Xinlu Zhang, Yujie Lu, Weizhi Wang, An Yan, Jun Yan, Lianke Qin, Heng Wang, Xifeng Yan, William Yang Wang, and Linda Ruth Petzold. 2023. Gpt-4v (ision) as a generalist evaluator for vision-language tasks. *arXiv preprint arXiv:2311.01361* (2023).
- [79] Yiqun Zhao, Zibo Zhao, Jing Li, Sixun Dong, and Shenghua Gao. 2024. Roomdesigner: Encoding anchor-latents for style-consistent and shape-compatible indoor scene generation. In *3DV*. IEEE, 1413–1423.

- [80] Ting Zhou, Yanjie Zhao, Xinyi Hou, Xiaoyu Sun, Kai Chen, and Haoyu Wang. 2025. DeclarUI: Bridging Design and Development with Automated Declarative UI Code Generation. *PACMSE 2, FSE (2025)*, 219–241.
- [81] Xiaoyu Zhou, Xingjian Ran, Yajiao Xiong, Jinlin He, Zhiwei Lin, Yongtao Wang, Deqing Sun, and Ming-Hsuan Yang. 2024. Gala3d: Towards text-to-3d complex scene generation via layout-guided generative gaussian splatting. *arXiv preprint arXiv:2402.07207 (2024)*.